Jurnal Polimesin
Department of Mechanical Engineering
State Polytechnic of Lhokseumawe
http://e-jurnal.pnl.ac.id/polimesin
e-ISSN : 2549-1999 No. : 1 Month : February
p-ISSN : 1693-5462 Volume : 23 Year : 2025

Processing dates: received on 2024-09-15, reviewed on 2024-11-20, accepted on 2025-1-11 and online availability on 2025-02-28

Performance evaluation of helix and spiral receiver geometries for a parabolic solar collector using CFD Analysis

Ahmad Yonanda[1,*], Naufal Hakim[1], Amrizal[1], Muhammad Irsyad[1], Harmen[1], Akhmad Riszal [1], and Jorfri Boyke Sinaga[1], Muhammad Haviz[2]

[1] Department of Mechanical Engineering, University of Lampung Bandar Lampung 35141, Indonesia.

[2] Department of Chemical Engineering, KFUPM, Dhahran 31261, Saudi Arabia

* Corresponding author: ahmad.yonanda@eng.unila.ac.id

Abstract

This comparative study evaluates the thermal performance of helix and spiral-shaped receivers in a Parabolic Dish Collector (PDC) system, a renewable energy technology that converts solar radiation into heat by concentrating sunlight onto a receiver. The geometry of the receiver significantly influences heat absorption and system efficiency. Using Computational Fluid Dynamics (CFD) simulations, this research compares temperature distribution, fluid flow velocity, and thermal energy transfer between the two receiver designs. Results indicate that the helix receiver provides more uniform heat distribution and achieves 2.6% higher thermal efficiency than the spiral receiver. However, the spiral receiver exhibits higher central flux and benefits from a simpler design and lower production costs. These findings offer insights into selecting optimal receiver geometries for improved solar energy utilization, supporting the advancement of efficient parabolic solar collector technology in renewable energy applications.

Keywords:

Parabolic Dish Collector (PDC), receiver geometry, Computational Fluid Dynamics (CFD), thermal performance, lower costs.

1 Introduction

In the last decade, the development of renewable energy has been continuously optimized to reduce the use of fossil fuels. One of the most popular renewable energy sources today is solar energy. As a country located on the equator, Indonesia has a greater opportunity to harness solar energy, both in quantity and quality, compared to regions not crossed by the equator. Indonesia has a solar energy potential of about 4.8 kWh/m or equivalent to 112,000 GWp, and this solar energy will continue to be available over time [1-2]. The use of solar energy in Indonesia is an appropriate choice as an alternative energy source for industrial energy needs or to meet daily energy demands, both in industry and households. One technology that utilizes solar energy is Concentrated Solar Power (CSP), commonly known as concentrated solar power plants. One of the most popular CSP types is the Parabolic Dish Collector (PDC). PDC is designed using mirrors or reflective materials in the form of a large dish, intended to capture and reflect sunlight (or other electromagnetic waves) towards a receiver installed at the focal point [3-5].

The receiver is a component that contains a working fluid, which can then be further utilized, such as to drive a steam turbine for electricity generation. In its application, the PDC has a drawback: when solar radiation is focused on the receiver, not all of the sunlight is absorbed optimally by the receiver due to several factors, such as material selection, focus point placement configuration, and the geometry or dimensions of the receiver. This research focuses on the impact of receiver dimensions on the performance of the working fluid temperature generated using an open-flow system. Several studies on the use of receiver dimensions have been conducted by previous researchers, [6] studied the influence of different cylindrical receiver dimensions by comparing four types of cylindrical receivers with different diameters and heights using the Computational Fluid Dynamic (CFD) simulation method. In that study, the variation in cylindrical receiver dimensions affected the fluid temperature distribution and heat flux within the receiver. It was found that cylindrical receivers with lower heights had higher thermal efficiency compared to taller cylindrical receivers. Then, [7-9] researched and simulated a cylindrical receiver with a spiral pipe inside. From that study, it was concluded that the spiral pipe affects the fluid flow pressure, temperature distribution, and fluid flow velocity. The researcher [10-12] found that a receiver with cylindrical-conical geometry had 4% higher thermal efficiency compared to a rectangular geometry receiver and 13% higher compared to a spherical receiver.

In addition to research on the impact of receiver dimensions, studies have also been conducted on the addition of fins to the receiver pipes. For instance, research [13-17] examined flat-surfaced receivers and modified them with square tubular fins. It was proven that the addition of square tubular fins to the receiver could improve the performance and thermal efficiency of PDC by 71%. The addition of fins to the receiver enhances heat transfer to the fluid by minimizing heat loss, and the research used a modified spiral receiver with added fins. Apart from adding fins, the use of cavities has also been explored. They studied a coupled conical cavity receiver designed with a hollow cone shape, and this type of receiver increased optical-thermal performance by 4% for heating the fluid inside the receiver [17-19].

Based on previous studies, it has been proven that the design of receivers significantly affects the performance of PDC systems. However, despite various studies conducted on the influence of receiver geometry, there is still a lack of understanding regarding the comparison between helix and spiral shapes under different mass flow rate conditions. In this study, the thermal performance of helix and spiral receivers is simulated using the CFD approach with Ansys Fluent. The simulation involves varying mass flow rates of 0.01 kg/s, 0.02 kg/s, and 0.03 kg/s.

This simulation study is structured comprehensively and summarized in four sections. Section 1 provides the background and the necessity of designing solar receivers that offer optimal performance. Section 2 discusses the simulation methodology used in the research. Section 3 details the analysis of the working fluid temperature performance, which is significantly enhanced in this study. Section 4 summarizes the key conclusions obtained from this study and provides recommendations for further research.

2 Research methods

The simulation method for analyzing the performance of receivers in PDC is conducted using CFD software (Ansys Fluent version 24). The models in this study use two types of receivers: helix and spiral, intending to analyze the most optimal thermal performance based on working fluid temperature with varying mass flow rates. This study also examines the use of molten salt as a working fluid in relation to the thermal performance of the receiver. The configuration of the PDC system is set according to environmental conditions, where the irradiation received by the PDC is 1000 W/m², the ambient temperature is assumed to be 26°C, and the sun's position is perpendicular at 90° to the PDC. In this case, wind speed is neglected. For more details, see Fig. 1.

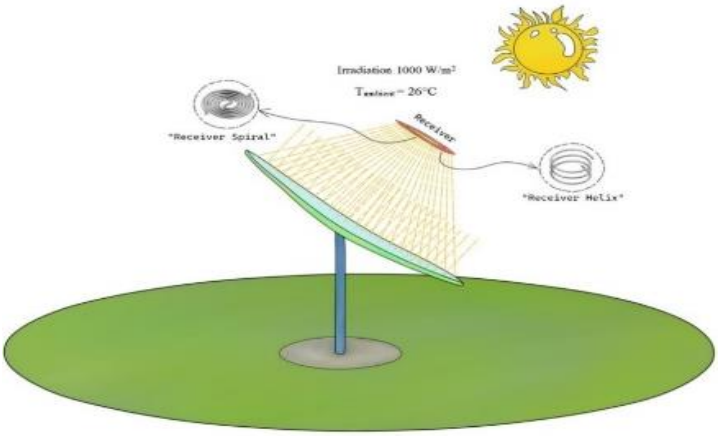

Fig. 1. The configuration Parabolic dish concentrator with a receiver.

2.1 Geometry modeling

The first step is to create a geometric model of the PDC system, including the parabolic dish and the receiver. This geometry can be created using CAD (Computer-Aided Design) software. The design of the reflector used in the PDC system consists of six sheets, each of which contains reflector facets. These facets are arranged in such a way as to cover the parabolic surface. The material of the facets is a 2 mm thick mirror, with a reflectivity level of R=0.9. The geometric shape of the parabolic dish can be seen in Fig. 2.

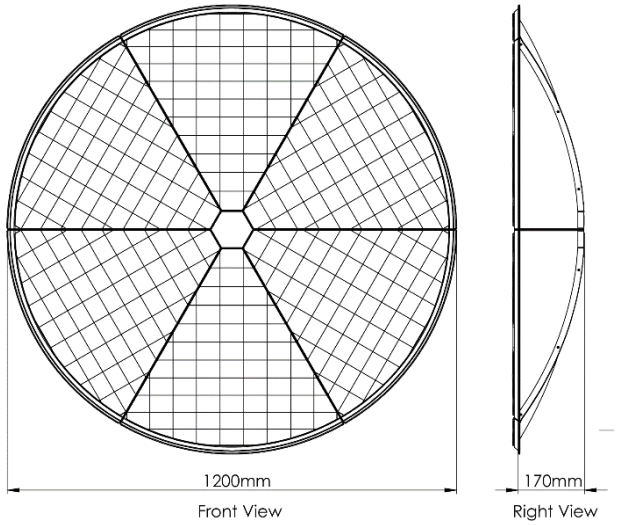

Fig. 2. The dimensions of the PDC and the arrangement of the mirrors

In Fig. 3(a), the dimensions of the spiral receiver are shown, while Fig. 3(b) depicts the helix receiver. Both receivers have an inner pipe diameter of 10 mm and an outer diameter of 12 mm. To compare the two receiver geometries, a pipe length of 2000 mm is used for both. Additionally, the receiver material is copper, which has high thermal absorption properties.

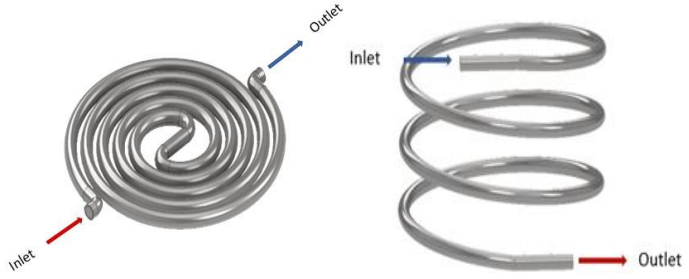

(a) (b)

Fig. 3. The direction of fluid flow entering the receiver: (a) spiral (b) helix.

2.2 Mesh modeling

In this study, the illustrates the mesh application on a spiral-shaped and helix receiver using a polyhexcore mesh type. The left side shows the overall structure of the helix receiver, while the right side zooms into the receiver pipe wall area to highlight the details of the mesh used. In the pipe wall region, boundary layer meshing is applied to accurately capture the effects of fluid flow and heat transfer near the surface. The polyhexcore mesh type is selected for its capability to handle complex geometries like the helix, ensuring flexibility and computational efficiency. Local refinement around the pipe wall enhances accuracy in critical regions without significantly increasing the overall number of mesh cells (Fig. 4).

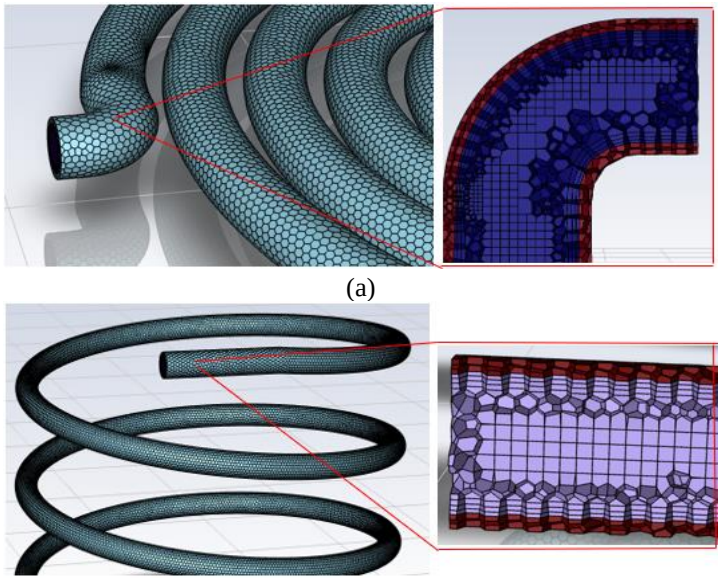

(a) (b)

Fig. 4. Polyhexcore Mesh Type for Receiver Geometry; (a) spiral and (b) helix

2.3 Computational modeling

The conjugate heat transfer in the PDC receiver encompasses both solid and fluid regions. The fluid, which is water, carries heat within the receiver pipe and then exits the system. The behavior of the fluid is governed by the fundamental principles of mass conservation, momentum conservation, and energy conservation. These principles can be expressed as a set of mathematical expressions known as the Navier-Stokes Eqs [1-3].

Continuity:

$$\frac{\partial \rho}{\partial t} + \nabla \cdot (\rho \vec{v}) = 0 \tag{1}$$

Moment:

$$\frac{\partial}{\partial t}(\rho \vec{v}) = -\nabla p + \nabla \cdot (\bar{\tau}) + \rho \vec{g} \tag{2}$$

Energy:

$$\frac{\partial}{\partial t}(\rho E) + \nabla \cdot \left(\vec{v}(\rho E + P)\right) = -\nabla \cdot \left(\sum_j h_j J_j\right) \tag{3}$$

In this context, ρ represents the density, p is the static pressure, τ is the stress tensor, ν denotes velocity, E stands for energy, h is the enthalpy of the species, and J refers to the diffusion flux. The governing equations are discretized through the standard finite volume method, resulting in a system of algebraic equations that are solved iteratively using CFD software. Meanwhile, the turbulent kinetic energy is given by Eq. 4:

$$\frac{\partial}{\partial t}(\rho k) + \frac{\partial}{\partial x_i}(\rho k u_i) = \frac{\partial}{\partial x_j}\left(a_k \mu_{eff} \frac{\partial k}{\partial x_j}\right) + G_k - \rho\varepsilon \tag{4}$$

Where G_k denotes the generation of turbulent kinetic energy caused by the gradient of the mean velocity. α_k, and α_ε are the inverse of the Prandtl numbers for k and ε.

2.4 Simulation process

The CFD process is simulated using Ansys 2024 R1. Before performing the CFD simulation, the irradiation received by the receiver is first calculated using Tonatiuh Solar Ray Tracing software. In this research case, a solar ray tracing value of 1000 W/m² is used, which is directed towards the parabolic dish. This irradiation will be reflected and concentrated on the receiver, increasing the irradiation value that reaches the receiver. To observe the effects of photon light rays on the receiver, simulations using Tonatiuh Solar Ray Tracing software are necessary . Tonatiuh is an open-source Monte-Carlo Ray™ Tracer (MCRT) software [22] for the optical simulation of solar concentrating systems. In this work, a PDC and a target surface (receiver) placed at its focus will be simulated, like PDC research by Ferero [23].

During the running setup phase in the solar ray tracing software, a scheme of solar light or heat irradiation to the PDC will be obtained, which is then reflected and directed towards the receiver. Fig. 5 shows the scheme for a spiral solar rays receiver, with heat from solar irradiation depicted by yellow lines or photon light rays. This running setup phase will produce output data in the form of irradiation values for each photon light ray effect, which can be calculated and processed to determine the total irradiation on the receiver.

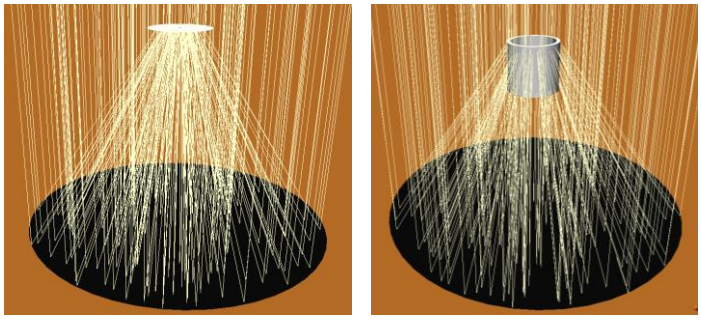

(a) (b)

Fig. 5. Solar rays receiver scheme: (a) spiral (b) helix

Table 1. Boundary conditions simulation (Fig. 6).

Boundary conditions	Value
CFD Model	k-ε Turbulence Model
Solar irradiance	1000 W/m^2
Ambient temperature	30 °C
Type fluid flow	Water (H_2O)
Mass flow rates	0.01, 0.02, 0.03 kg/s
Receiver geometry	Helix and spiral
Receiver surface emissivity	0.8
Wind speed around	Negligible
Solver settings	Steady-state simulation
	Energy Eq. activated
	Pressure-velocity coupling: COUPLE

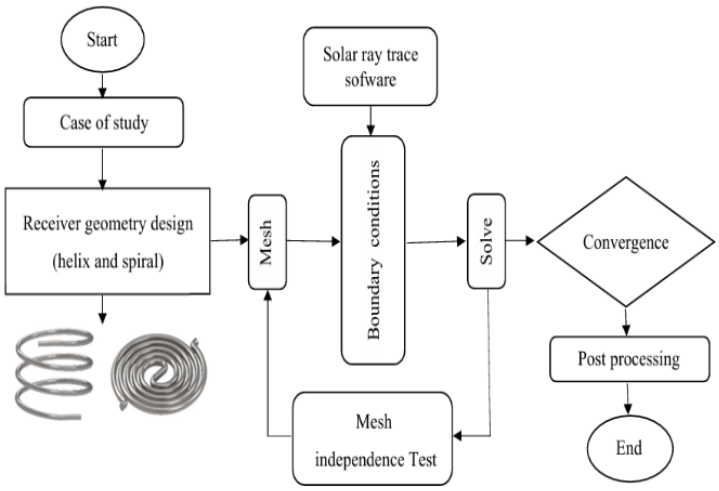

Fig. 6. The stages of the solar receiver simulation process

Boundary conditions in the simulation are necessary to avoid deviations in input parameters and to narrow the focus of the problem, ensuring that the research is more directed and facilitating the discussion, thus achieving the research objectives. In this simulation, a constant radiation value of 1000 W/m² is absorbed in PDC, along with variations in fluid types (water (H_2O) and variations in mass flow rates 0.01 kg/s, 0.02 kg/s, and 0.03 kg/s.

2.5 Mesh Independence Test (MIT)

In this study, five different mesh sizes were used, resulting in varying numbers of meshes. However, despite the differences in mesh quantity and size, the quality of the mesh for all five variations was maintained. These mesh sizes are categorized into large, medium, and small, with the smallest size resulting in the highest number of meshes. The PDC receiver was simulated with each of these mesh sizes using Ansys Fluent. After conducting the simulations, five datasets were obtained to evaluate mesh quality. The results are presented in the Table 2.

Table 2. Compares the outlet temperature of the fluid for the spiral and helix receivers against the mesh type

Mesh Type	Geometry Receiver	Number of Elements	T_{out} ℃
Coarse mesh	Spiral	144,417	236.2
	Helix	119,750	251.3
Medium Mesh	Spiral	454,700	235.1
	Helix	291,131	250,1
Refined Mesh	Spiral	503,819	233.9
	Helix	687,040	248.8
Very Refined Mesh	Spiral	1,111,039	233.9
	Helix	1,607,634	248.8

With five different mesh sizes, five varying mesh counts were obtained for each simulation. The data used for mesh verification were based on the simulation results of the outlet fluid temperature for both the spiral and helix receivers. As shown in Fig. 7, a mesh count of 503,819 yielded an outlet temperature of 233.92ºC for the spiral receiver. Increasing the mesh count to 755,328 and up to 1,111,039 cells still resulted in the same temperature of 233.92ºC. This indicates that using 503,819 cells provides results equivalent to those with 1,111,039 cells but with significantly less computational effort. Therefore, the optimal mesh size of 503,819 cells was chosen to simplify the iteration process while obtaining the outlet temperature results for the spiral receiver. This conclusion is specific to the temperature calculations of the spiral receiver in this study.

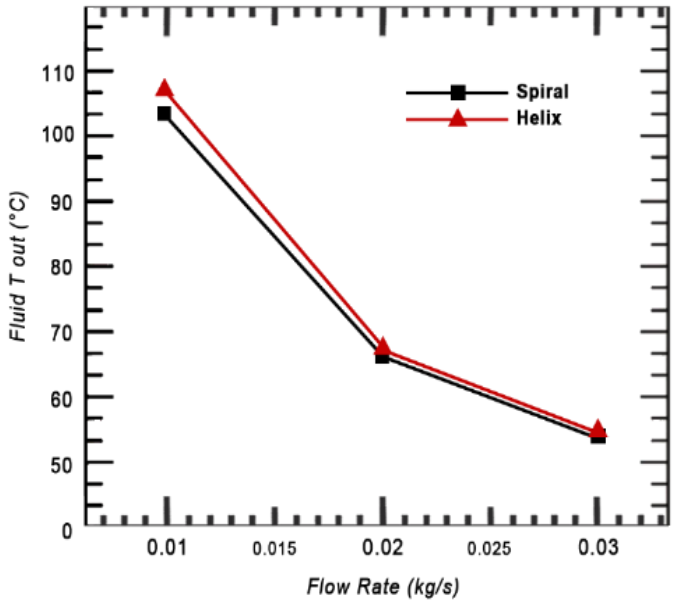

Fig. 7. Comparison graph of the outlet temperature of helical and spiral receivers with water fluid versus flow rate.

3 Results and Discussion

This study is conducted to determine the outlet temperature (T_{out}) of the fluid in the receiver, and the pressure drop of the fluid in the receiver, This study also involves variations in mass flow rates with respect to the outlet temperature of the fluid in the receiver, as well as variations in the geometry of the receiver with helical and spiral shapes to obtain a sufficiently optimal receiver design for achieving the desired fluid outlet temperature in the PDC.

3.1 The Effect of receiver geometry type on the outlet temperature of water fluid

In this study, two types of receivers, spiral and helical, were chosen for comparison to determine which receiver is most optimal for use in a PDC. The optimal receiver for a PDC is one that can increase the outlet temperature of the fluid, thereby enhancing the performance of the PDC. This study uses water as the working fluid, and variations in the fluid will be discussed in the following sections.

In the case of water fluid, as shown in Fig. 7, both the spiral and helical PDC receivers exhibit decreased performance in terms of outlet temperature as the flow rate increases. For a flow rate of 0.03 kg/s, the average decrease in temperature between the helical and spiral receivers from a flow rate of 0.02 kg/s is only 12.78°C. The most significant decrease occurs in the mass flow rate from 0.01 kg/s to 0.02 kg/s, where the temperature drop is twice as much compared to the drop from a mass flow rate of 0.02 kg/s to 0.03 kg/s. This is due to the fact that as the flow rate decreases, the fluid flow inside the receiver becomes slower, resulting in longer heat transfer contact between the receiver pipe and the fluid, which optimizes fluid heating.

The fluid is most optimal at the lowest flow rate of 0.01 kg/s because the fluid moves the slowest at this rate and has the longest contact time with the receiver pipe. When the flow rate is increased to 0.02 kg/s, the fluid moves faster, leading to shorter heating contact time with the receiver pipe and a significant decrease in temperature. However, between the two PDC receivers, the helical receiver consistently has a superior outlet temperature compared to the spiral receiver at every flow rate. Ata flow rate of 0.01 kg/s, the temperature difference (ΔT) of the outlet fluid is 2.75°C, with the helical receiver being more advantageous. The use of the helical receiver results in a 2.64% increase in outlet fluid temperature compared to the spiral receiver.

There is no significant difference in the outlet temperature (ΔT) of the fluid between the helical and spiral receiver geometries when using water fluid. However, if examined in detail, the ΔT of the outlet fluid in both helical and spiral receivers decreases as the flow rate increases. For instance, at a flow rate of 0.01 kg/s, the ΔT is 2.75°C; at a flow rate of 0.02 kg/s, the ΔT is 0.48°C; and at a flow rate of 0.03 kg/s, the ΔT is 0.19°C. This decrease in ΔT is due to the uneven exit of the fluid at the outlet of the spiral receiver pipe, where the fluid only exits from some parts of the outlet pipe. As the flow rate increases, the fluid in the spiral receiver exits more evenly. This is due to the spiral receiver's geometry, which has many curves or bends; this phenomenon will be explained in more detail with the fluid outlet contour of the spiral receiver in the following section. In contrast, the helical receiver allows the fluid to exit more uniformly at the pipe outlet. The uneven exit of fluid at the spiral receiver outlet affects the outlet temperature of the fluid, which is why the helical receiver has a superior outlet temperature compared to the spiral receiver.

3.2 Fluid Temperature Contour in Helical and Spiral Receivers.

The contour is used in this simulation because it can represent the desired values of an object. Contours can show temperature, pressure, and even velocity values. In this study, several contours are displayed, such as fluid flow temperature contours and fluid flow behavior contours.

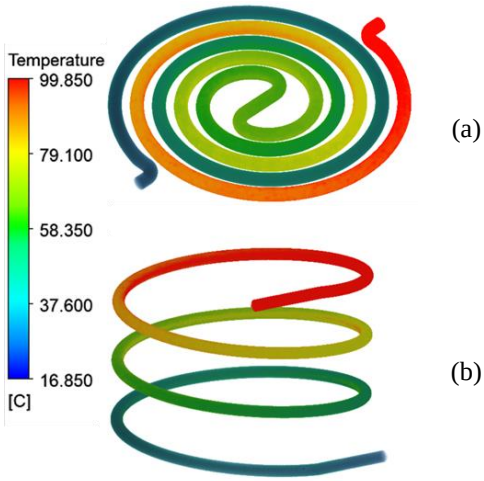

Fig. 8. The fluid temperature contour of water with a flow rate of 0.01 kg/s on the receiver: (a) Spiral (b) Helix

The contour with red color indicates higher temperature values, while lower temperatures are depicted with gradient contours ranging from blue to green. These colors provide a visual representation of the temperature distribution in the fluid, making it easier to identify areas with high or low temperatures. Figure 8 illustrates the temperature distribution of the fluid across the entire section of the helix and spiral receivers, using water as the working fluid at the lowest mass flow rate of 0.01 kg/s.

In the spiral receiver, the red contour at the outlet indicates that the fluid outlet temperature has reached 100.1°C. This temperature is significant because it is at the maximum of the liquid phase of water under standard atmospheric pressure conditions. Achieving this temperature shows that the spiral receiver is capable of efficiently absorbing and transferring heat energy from the receiver surface to the working fluid. This process also indicates that the spiral geometry provides a uniform heat distribution across the fluid, although there are slight variations represented by the color gradient in the outlet area. On the other hand, in the helix receiver (if mentioned in the subsequent section), the temperature distribution may vary depending on the more complex geometry and more turbulent fluid flow. However, the primary focus of this analysis is the spiral receiver's ability to utilize low flow rates and generate high temperatures close to the water's saturation point, without causing an undesirable phase transition from liquid to vapor under certain conditions.

This temperature distribution reflects the overall thermal efficiency of the system, where achieving temperatures close to 100°C can be optimized for thermal energy applications, such as steam production for turbines or other industrial processes

.

3.3 Contours of Fluid Flow Behavior at the Receiver Outlet

The fluid flow contours in this study are displayed to closely observe the behavior of fluid flow at the outlet of the receiver pipe, which can influence the fluid outlet temperature. Fluid flow behavior refers to the way the fluid moves and interacts with its surroundings. Fluid flow can be highly complex, and its behavior depends on various factors such as viscosity, flow velocity, the shape of the container, and forces acting on the fluid.

In this research, the primary factor causing differences in flow behavior is the shape of the fluid container, or the geometry of the receiver, whether helix or spiral. The impact of varying receiver geometry on fluid flow behavior must also be considered, as the flow behavior at the receiver, particularly at the outlet of both the helix and spiral receivers, will certainly affect the fluid outlet temperature from the receiver.

Fig. 9 shows the phenomenon observed in the spiral and helix receivers can be explained by the differences in the geometry of these two types of receivers. The spiral receiver has many bends or sharp turns, which prevent the fluid from exiting uniformly at the

outlet. These sharp turns disrupt the fluid flow and create turbulence, leading to uneven temperature distribution at the outlet. This affects the system's efficiency, as the temperature difference between the faster and slower fluid flows will influence the overall heat transfer. On the other hand, the helix receiver has a smoother geometry and more stable fluid flow, allowing for more even temperature distribution at the outlet, even with varying flow rates.

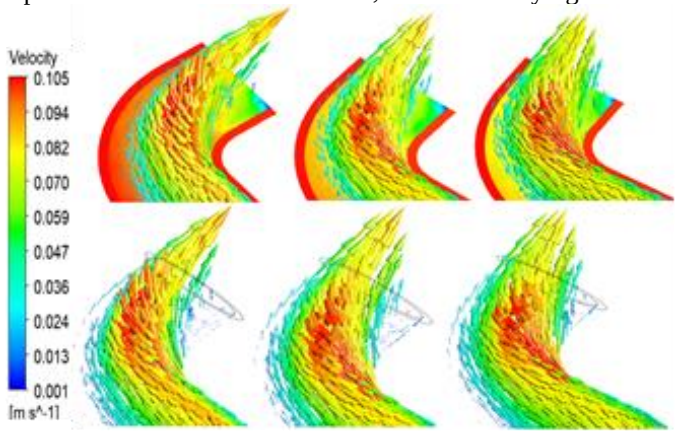

(a) (b) (c)

Fig. 9. The vector of fluid flow velocity at the outlet of the spiral receiver at specific flow rates: (a) 0.01 kg/s, (b) 0.02 kg/s (c) 0.03 kg/s

As the flow rate increases, the fluid in the spiral receiver tends to exit more uniformly, though it is still less efficient than the flow in the helix receiver. The increase in flow rate causes a decrease in the temperature difference (ΔT) at the fluid outlet in both types of receivers, although this decrease is more optimal in the helix receiver, which maintains a more consistent flow. The spiral geometry, with its sharp turns, remains the main obstacle, preventing the fluid flow from achieving maximum efficiency. Therefore, the helix receiver demonstrates better performance in terms of flow distribution and outlet fluid temperature, making it a superior choice for applications that require high efficiency.

Overall, the helix receiver has a significant advantage in terms of efficiency and uniform temperature distribution compared to the spiral receiver. Although the spiral receiver can show improvement in fluid flow distribution with an increased flow rate, its more complex geometry with many sharp turns remains the main obstacle to achieving optimal performance. With a more stable geometry and more consistent fluid flow, the helix receiver can maintain better performance in terms of temperature distribution and overall system efficiency.

The detailed capture of the fluid outlet surface is also shown to observe its temperature distribution. Fig. 10 shows the temperature contours of water at the outlet of the helix and spiral receivers, respectively, each with its characteristics due to the behavior of fluid flow at the pipe outlet. In the spiral receiver, some parts of the fluid contour still show a low temperature of 26˚C. This is due to the uneven fluid exit at the outlet of the spiral receiver, caused by the spiral receiver's geometry. Therefore, selecting the appropriate receiver geometry in a PDC is crucial, as the geometry acts as the container shape for the working fluid, influencing the fluid flow behavior within the receiver. This, in turn, impacts the receiver's performance; the higher the fluid outlet temperature from the receiver, the better the receiver's performance.

(a) (a)

(b)

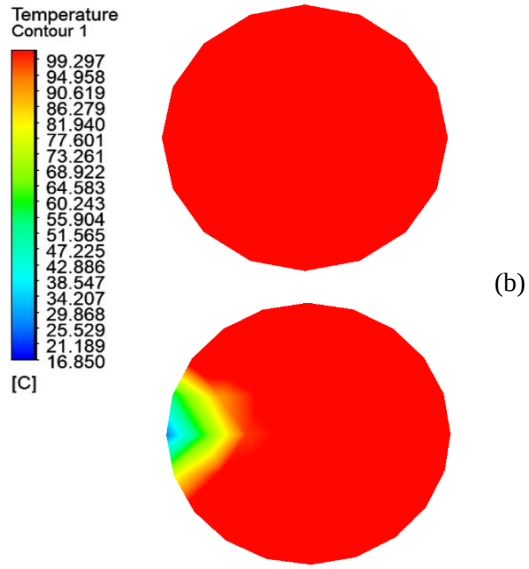

Fig. 10. The temperature contour of water at the outlet receiver (a) Spiral and (b) Helix

3.4 Analysis of Reynold Number and Nusselt Number

The comparison of the Reynolds number to the Nusselt number helps illustrate the efficiency of heat transfer as the flow characteristics change. Reynolds number (*Re*) is a dimensionless parameter that facilitates the prediction of flow behavior.

On the other hand, Nusselt number (*Nu*) can be defined as the ratio of convective heat transfer to conductive heat transfer within the fluid under the same conditions. Fig. 11 illustrates that an increase in Reynolds number in both the helix and spiral receivers leads to a higher Nusselt number. For water as the fluid, the highest Reynolds number is found in the helix receiver at 5,272.69, while the highest Nusselt number is also in the helix receiver at 22.29.

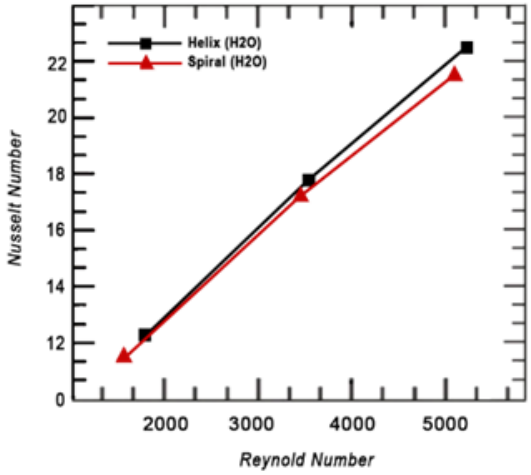

Fig. 11. The graph compares Reynolds Number (*Re*) and Nusselt Number (*Nu*) for the helix and spiral receivers.

The increase in Nusselt number with the increase in Reynolds number indicates that convective heat transfer becomes more dominant compared to conductive heat transfer. Therefore, it can be explained that increasing the Reynolds number to reach the turbulent flow stage significantly enhances the Nusselt number, meaning that convective heat transfer becomes much more dominant compared to conduction.

The increase in Reynolds number in both the helix and spiral receivers leads to a higher Nusselt number, indicating that convective heat transfer becomes more dominant compared to conduction. The helix receiver shows better performance with the highest Reynolds and Nusselt numbers, suggesting that the more stable turbulent flow in the helix receiver significantly enhances heat transfer efficiency.

4 Conclusion

The fluid outlet temperature serves as a key performance indicator for receiver efficiency. The helix receiver outperforms the spiral receiver, producing a 2.64% higher fluid outlet temperature at the lowest flow rate (0.01 kg/s). Both receiver geometries exhibit a decline in outlet temperature as flow rate increases, indicating that fluid flow rate significantly impacts thermal performance. While the helix receiver enhances heat distribution and efficiency, the spiral receiver offers advantages in design simplicity and cost-effectiveness. These findings contribute to optimizing receiver geometry selection for parabolic dish collector applications, promoting advancements in solar thermal energy systems.

References

[1] Kementerian Energi dan Sumber Daya Mineral (KESDM). (2024) Utilization of Solar Energy in Indonesia. Available at: https://www.esdm.go.id/id/media-center/arsip-berita/pemanfaatan-energi-surya-di-indonesia (Accessed: 27 August 2024).

[2] Arif Nugroho, A. (2017). Pembangkit Listrik Tenaga Surya Menggunakan Stirlling Engine. Pengembangan Insfrastruktur dan Technopreneurship Untuk Meningkatkan Daya Saing Bangsa, 5–8. https://doi.org/10.21063/PIMIMD4. 2017.6-10

[3] Breeze, P. (2016). Solar Towers. Dalam Solar Power Generation (hlm. 35–40). Elsevier. https://doi.org/10.1016/b978-0-12-804004-1.00005-1

[4] Nallaperumal, T. N., Sellapandiyan, R. K., Vishnu, S. K., & Senthil, R. (2024). Numerical and experimental analysis of a cross-finned solar receiver for parabolic dish collectors. Applied Thermal Engineering, 248. https://doi.org/10.1016/j.applthermaleng.2024.123329

[5] Rajan, A., & Reddy, K. S. (2024). Integrated optical-thermal model and deep learning technique to estimate the performance of a conical cavity receiver coupled solar parabolic dish collector. Energy Conversion and Management, 301. https://doi.org/10.1016/j.enconman.2023.118052

[6] Cherif, H., Ghomrassi, A., Sghaier, J., Mhiri, H., & Bournot, P. (2019). A receiver geometrical details effect on a solar parabolic dish collector performance. Energy Reports, 5, 882–897. https://doi.org/10.1016/j.egyr.2019.07.010

[7] Pratik, N. A., Ali, M. H., Lubaba, N., Hasan, N., Asaduzzaman, M., & Miyara, A. (2024). Numerical investigation to optimize the modified cavity receiver for enhancement of thermal performance of solar parabolic dish collector system. Energy, 290. https://doi.org/10.1016/j.energy.2023.130133

[8] Bellos, E., Bousi, E., Tzivanidis, C., & Pavlovic, S. (2019). Optical and thermal analysis of different cavity receiver designs for solar dish concentrators. Energy Conversion and Management: X, 2. https://doi.org/10.1016/j.ecmx. 2019. 100013

[9] Dabiri, S., & Rahimi, M. F. (2016). Introduction of solar collectors and energy and exergy analysis of a heliostat plant The 3rd International Conference and Exhibition on Solar Energy Basic introduction of solar collectors and energy and exergy analysis of a heliostat plant. https://www.researchgate. net/publication/318360867

[10] Hamdah Husniyyah, H., & Ayodha Ajiwiguna, T. (2019). ANALISIS EFISIENSI PADA CONCENTRATED SOLAR THERMAL COLLECTOR TIPE PARABOLIK EFFICIENCY ANALYSIS OF PARABOLIC CONCENTRATED SOLAR THERMAL COLLECTOR.

[11] Hasbi Assiddiq, & Irma Dinahkandy. (2018). Studi pemanfaatan energi matahari sebagai sumber energi alternatif terbarukan berbasis sel fotovoltaik untuk mengatasi kebutuhan listrik rumah sederhana di daerah terpencil. Al-jazari jurnal ilmiah teknik mesin, 3(2). https://doi.org/10.31602/al-jazari.v3i2.1624

[12] Islam, M. T., Huda, N., Abdullah, A. B., & Saidur, R. (2018). A comprehensive review of state-of-the-art concentrating solar power (CSP) technologies: Current status and research trends. Dalam Renewable and Sustainable Energy Reviews (Vol. 91, p. 987–1018). Elsevier Ltd. https://doi.org/10.1016/j. rser.2018.04.097

[13] Joardder, M. U. H., Halder, P. K., Rahim, M. A., & Masud, M. H. (2017). Solar pyrolysis: Converting waste into asset using solar energy. Dalam Clean Energy for Sustainable Development: Comparisons and Contrasts of New Approaches (hlm. 213–235). Elsevier Inc. https://doi.org/10.1016/B978-0-12-805423-9.00008-9

[14] Kurnia, A., & Rahmalina, D. D. (2021). Proses Simulasi Sistem Concentrated Solar Power Equipment Simulation Process of Concentrated Solar Power Equipment. 3, 115–122.

[15] Rizki Ikhsan, M., Rizali, M., & Nugraha, B. (2024). SIMULASI CFD UDARA DI SEKITAR RUMAH TRADISIONAL BANJAR TIPE BUBUNGAN TINGGI AIR CFD SIMULATION AROUND TRADITIONAL HIGH-RIDGE TYPE BANJAR HOUSE. 6, 2721–6225. https://doi.org/10.20527/jtamrotaryv7i1.216

[16] Sari, C. P., Fadhilah*, R., & Kurniasih, D. (2022). Validitas Alat Praktikum Kimia Berbasis Bahan Bekas pada Materi Termokimia. Jurnal IPA & Pembelajaran IPA, 6(2), 130–144. https://doi.org/10.24815/jipi.v6i2.24907

[17] Vengadesan, E., Gurusamy, P., & Senthil, R. (2023). Thermal performance analysis of flat surface solar receiver with square tubular fins for a parabolic dish collector. Renewable Energy, 216. https://doi.org/10.1016/j.renene. 2023. 119048

[18] Vishnu, S. K., & Senthil, R. (2023). Experimental performance evaluation of a solar parabolic dish collector using spiral flow path receiver. Applied Thermal Engineering, 231. https://doi.org/10.1016/j.applthermaleng.2023.1209

[19] Amin, M., Rizal, T.A., Amir, F., Abdullah, N.A. and Ginting, S.F. (2023), An experimental study on parabolic trough solar cookers with materials collector of chrome stickers and glass mirrors, Journal Polimesin, 21(5), p. 4521. doi: 10.30811/jpl.v21i5.4521.

[20] Yonanda, A., Amrizal, Harmen, H., Riszal, A. and Ibrahim, F. (2022) 'Photovoltaic (PV) thermal performance simulation using segmentation lapping fin passive cooling', Journal Polimesin, 20(2), p. 3041. doi: 10.30811/jpl.v20i2.3041.

[21] Cengel, Y. A. (2003). Heat Transfer A Practical Approach, Second Edition

. www.TechnicalBooksPdf.comwww.TechnicalBooksPdf.com

[22] Blanco MJ, Amieva JM, Mancillas A. The Tonatiuh software development project: An open source approach to the simulation of solar concentrating systems. In: ASME 2005 international mechanical engineering congress and exposition. American Society of Mechanical Engineers; 2005, p. 157–64. https://doi.org/10.1115/IMECE2005-81859

[23] J. García Ferrero, R.P. Merchán a, M.J. Santos, A. Medina, A. Calvo Hernández a, P. Canhoto b, A. Giostri c. Modeling a solar pressurized volumetric receiver integrated in a parabolic dish: Off-design heat transfers, temperatures, and efficiencies. https://doi.org/10.1016/j.enconman.2023.117436

[24] Belkacem Kada, Shahid, Amjad Ali Pasha, Fayyaz Ahmad, Muhammad Suleman, Waqar Azeem Khan. Analysis of flow and heat transfer in bend pipe with different smoothing.https://doi.org/10.1016/j.icheatmasstransfer.2024.107924Get rights and content